LAWRENCE
LIVERMORE
NATIONAL
LABORATORY

LLNL-JRNL-562754

Distinct Effects of Reduced Sulfur Compounds on Pd-catalytic Hydrodechlorination of TCE in Groundwater Using Cathodic H2 under Electrochemically-induced Oxidizing Conditions

S. Yuan, M. Chen, X. Mao, A. N. Alshawabkeh

June 28, 2012

ENVIRONMENTAL SCIENCE & TECHNOLOGY

Disclaimer

Distinct Effects of Reduced Sulfur Compounds on Pd-catalytic Hydrodechlorination of TCE in Groundwater Using Cathodic H_2 under Electrochemically-induced Oxidizing Conditions

Songhu Yuan[†,‡], *Mingjie Chen*[§], *Xuhui Mao*[‡] *and Akram N. Alshawabkeh* [*,‡]

[†]State Key Lab of Biogeology and Environmental Geology, China University of Geosciences, 388 Lumo Road, Wuhan, 430074, P. R. China

[‡]Department of Civil and Environmental Engineering, Northeastern University, 400 Snell Engineering, 360 Huntington Avenue, Boston, Massachusetts 02115, United States

[§]Atmospheric, Earth and Energy Division, Lawrence Livermore National Laboratory, P.O. Box 808, L-184, Livermore, CA 94550, United States

RECEIVED DATE (to be automatically inserted after your manuscript is accepted if required according to the journal that you are submitting your paper to)

* To whom correspondence should be addressed. E-mail: aalsha@coe.neu.edu (A. Alshawabkeh).

ABSTRACT Pd-catalytic hydrodechlorination of trichloroethylene (TCE) in groundwater using electro-generated H_2 is investigated under electrochemically-induced oxidizing condition. In particular, the distinct effects of sulfide and sulfite are elucidated. In an undivided electrolytic cell, TCE is hydrodechlorinated to ethane by Pd and cathodic H_2 even though anodic O_2 is proportionally generated. In a typical treatment at pH 4, TCE (26.1 mg/L) is hydrodechlorinated, in a pseudo-zero-order kinetics, by 67.7% within 80 min with the accumulation of 19.2 mg/L H_2O_2. Sulfide shows moderate inhibition on both TCE hydrodechlorination and H_2O_2 accumulation by foiling Pd catalyst. Different from the influence under anaerobic condition, sulfite at low concentrations ($\leq$ 1 mM) significantly enhances TCE decay, and at high concentration (3 mM) inhibits initially and enhances afterwards when sulfite concentration declines to less than 1 mM. Sulfite is oxidized by chemisorbed H_2O_2 and •OH forming $SO_3^{\bullet-}$ and $SO_5^{\bullet-}$ radicals, which contributes to TCE decay through oxidation in parallel to Pd-catalytic hydrodechlorination. Using a specially configured three-electrode column, acidic and oxidizing conditions are automatically developed in the Pd zone, wherein TCE is greatly hydrodechlorinated with certain resistance to RSC foiling.

INTRODUCTION

Contamination of groundwater by chlorinated hydrocarbon compounds (CHCs), such as trichloroethylene (TCE) and perchloroethylene (PCE), continues to be a

serious world-wide environmental problem.[1] Pd-catalytic hydrodechlorination is a process that is proposed and tested for transformation of CHC contamination. A variety of CHCs can be rapidly hydrodechlorinated to less toxic or nontoxic and more readily biodegradable substances.[2–8] Field applications prove that the performance of Pd-catalytic hydrodechlorination of CHCs by H_2 can be sustained for several years.[9–11] Typically H_2 is generally supplied as a compressed gas. Groundwater is saturated with H_2, and then passes through a Pd catalyst bed, wherein CHCs are hydrodechlorinated. However, there are a few barriers for full-scale implementation. Transportation and storage of compressed H_2 gas is dangerous, and injecting H_2 into subsurface is relatively costly. Furthermore, catalytic activity of Pd is significantly decreased in the presence of reduced sulfur compounds (RSCs) generated from anaerobic bacterial respiration in the aquifer.[5,9,11] Oxidizing reagents, such as hypochlorite,[5,9,12] hydrogen peroxide,[10] and permanganate,[13] can regenerate sulfur-fouled Pd catalyst to some extent. However, the periodical flushing of catalyst bed with oxidizing reagent complicates the operation. Therefore, it is crucial to seek new strategies to supply H_2 safely and expediently and to increase the resistance of Pd to RSC fouling.

Water electrolysis at a cathode (1) provides an alternative approach for supplying H_2 in situ. A preliminary investigation shows that TCE in groundwater could be hydrodechlorinated using H_2 produced by an undivided electrolyzer.[14] Our recent work also proves the feasibility of in situ supplying cathodic H_2 for 2,4-dichlorophenol hydrodechlorination in a divided electrolytic cell.[15] In both

investigations, the electrolytic system was the sole source of H_2, and the other products, i.e., O_2, from water electrolysis (2) were assumed to inhibit hydrodechlorination.[14,15] Nevertheless, production of O_2 at the anode is inevitable when water electrolysis happens. Recently, significant accumulation of H_2O_2 (> 20 mg/L) was detected in an undivided electrolytic cell in the presence of Pd catalyst under acidic condition (3), and low concentrations of strong oxidizing •OH radical (oxidation potential: 2.8 V vs standard hydrogen electrode, SHE) were also measured (4).[16,17] Reactive oxygen species (ROSs), i.e., H_2O_2, •OH and dissolved O_2, can oxidize RSCs in aqueous solution.[18–21] The efficient oxidation of sulfide in wastewater at mixed metal oxide coated titanium (Ti/MMO) electrode was recently evaluated.[22,23] As a result, when water electrolysis at inert electrodes, i.e., Ti/MMO, is used to supply H_2 for Pd-catalytic hydrodechlorination of CHCs in groundwater, Ti/MMO electrode and the simultaneously generated ROSs can potentially oxidize RSCs, thereby increasing the resistance of Pd to the fouling by RSCs.

$$2H_2O + 2e^- \longrightarrow H_2 + 2OH^- \quad (1)$$

$$2H_2O \longrightarrow O_2 + 4H^+ + 4e^- \quad (2)$$

$$H_2 + O_2 \xrightarrow{Pd} H_2O_2 \quad (3)$$

$$H_2O_2 \xrightarrow{Pd} 2\bullet OH \quad (4)$$

Since H_2O_2 and •OH are typically generated at weak acidic condition,[14,15] the H^+ and OH^- produced from water electrolysis the at electrodes (2–3) provide means to develop appropriate pH conditions in the reaction zone of Pd fillings. When one anode and two cathodes are arrayed properly in a column (See Figure 1 for details), it

is feasible to reach local low pH on Pd surface along with neutral effluent, making the generation of ROSs possible while adjusting the effluent to neutral pH conditions.

In this study, an undivided electrolytic cell is used to investigate the effect of RSCs, sulfide (sulfide and bisulfide) and sulfite (sulfite and bisulfite), on H_2O_2 generation and Pd-catalytic hydrodechlorination of TCE in simulated groundwater using H_2 produced by water electrolysis. As reactions differ greatly under oxidizing and reducing conditions, the mechanisms for the influence of RSCs at oxidizing conditions are elucidated. A three-electrode column is developed to reach low pH and oxidizing condition on Pd zone, thus generating ROSs for RSC oxidation. The column performance is tested in terms of TCE hydrodechlorination and RSCs resistance.

EXPERIMENTAL SECTION

Chemicals. TCE (99.5%) and cis-dichloroethylene (cis-DCE, 97%) were purchased from Sigma-Aldrich. H_2O_2 (30%) and Na_2SO_3 (98.1%) were purchased from Fisher Sci. $Na_2S•9H_2O$ (98%) and L-ascorbic acid sodium salt (99%) were obtained from Acros. 5,5-dimethyl-1-pyrroline-N-oxide (DMPO) was provided by Cayman Chemical Company (USA). Gas standard (1% (v/v) methane, ethene, ethane, acetylene, CO_2 and CO in nitrogen) was supplied by Supelco. Excess TCE was dissolved into 18.2 mΩ·cm high-purity water to form a TCE saturated solution (1.07 mg/mL at 20 ^oC), which was used as stock solution for preparing aqueous TCE solutions. Palladium on alumina powder (1% wt. Pd, Sigma-Aldrich) with average particle size of 6 μm was used as catalyst in batch experiments. Palladium on alumina

pellet (0.5% wt. Pd, Sigma-Aldrich) at much larger size of 3.2 mm (Figure S1 in Supporting Information, SI) was used in column experiments. Deionized water (18.0 mΩ·cm) obtained from a Millipore Milli-Q system was used in all the experiments. All chemicals used in this study were above analytical grade.

TCE Hydrodechlorination in an Undivided Electrolytic Cell. The same experimental setup as reported previously[17] is used for TCE hydrodechlorination at ambient temperature. As shown in Figure S2, a 150-mL syringe with plunge was connected to the cell, allowing gas expansion during electrolysis. Two pieces of Ti/MMO (coated with IrO_2/Ta_2O_5, mesh type, 3N International, USA) with dimension of 85 mm length by 15 mm width and 1.8 mm thickness were used as anode and cathode with 42 mm spacing in parallel position. For each test, 400 mL of 10 mM Na_2SO_4 solution was transferred into the cell, and 1 g/L Pd/Al_2O_3 were attained by addition of specific mass of Pd/Al_2O_3 powder. Na_2SO_3 powder and Na_2S stock solution were added, respectively. 10 mL of TCE saturated water was then added to produce an initial concentration of 198 μM (26.1 mg/L). The reactor was sealed immediately and the solution was stirred (600 rpm) for 10 min to allow equilibrium of TCE in the aqueous solution. A constant electric current of 100 mA (10 mA/cm^2) was applied with a cell voltage of about 7 V. The aqueous solution was sampled for analysis of TCE, *cis*-DCE, pH and H_2O_2 concentrations. Gas samples were collected from specific experiment for headspace gas analysis.

TCE Hydrodechlorination in a Column. A vertical three-electrode column (3.175 cm inner diameter × 30 cm length), as shown in Figure 1, was used to perform

flow-through experiments. Three pieces of TI/MMO mesh were installed in sequence as Cathodes 1, Anode and Cathode 2. 3 g of Pd/Al_2O_3 pellets were supported by Anode forming a monolayer of pellet bed. This dosage of the catalyst is packed because moderate removals of contaminants can be achieved for comparisons. A total current of 60 mA (7.6 mA/cm^2) was applied at Anode with the total voltage of about 20 V. By adjusting the rheostat, the cathodic current was equally partitioned in the two cathodes. No fillings were packed between Cathode 1 and Anode to reduce electric resistance. The remaining space in column was packed with 4-mm size glass beads with a porosity of 0.65. The total and pore volume (PV) are 245 and 160 mL, respectively. Simulated TCE-contaminated groundwater at 5.3 mg/L was prepared by dissolving TCE-saturated solution in 3 mM Na_2SO_4 and 0.5 mM $CaSO_4$ deoxygenated solution (~ 800 μS/cm), which was stored in gas-tight collapsing bag. Prior to electrolysis, the column was rinsed by 2 PVs of TCE-contaminated groundwater. Adsorption of TCE on Pd/Al_2O_3 pellets and glass beads was measured to be insignificant. The flow rate was maintained at 2 mL/min (0.25 cm/min) using a peristaltic pump (Cole Parmer). At regular time intervals, about 1 mL of groundwater were sampled from 6 ports (see Figure 1 for locations) for contaminant and pH measurement.

A total of 4 column experiments were carried out with parameters listed in Table S1. Column C1 gives the control removal without Pd, C2 measures TCE hydrodechlorination on Pd surface under electrochemically developed acidic and oxidizing conditions, and C3 and C4 evaluates the effect of sulfide and sulfite on TCE

hydrodechlorination.

Chemical analysis. TCE and cis-DCE concentrations were measured by a 1200 Infinity Series HPLC (Agilent) equipped with an 1260 DAD detector and a Thermo ODS Hypersil C18 column (4.6 × 50 mm). The mobile phase was a mixture of acetonitrile and water (60:40, v/v) at 1 mL/min. The detection wavelength was 210 nm. Ethene and ethane in the headspace were detected by Model 310 GC (SRI, USA) with flame ionization detector and Haysep-T column. 100 μL of headspace gas was sampled and injected from an on-column port. The temperature program includes heating the column from 40 to 140 ^{o}C at a rate of 15 ^{o}C/min, holding the temperature at 140 ^{o}C for 1 min, and then cooling to 40 ^{o}C at a rate of 20 ^{o}C/min. For the batch experiments, gas concentrations of TCE and aqueous concentrations of ethane were calculated by Henry's law, and the sum of aqueous and gas concentrations was derived.

Sulfite at concentration higher than 1 mM was also measured by HPLC using the same procedure as for TCE analysis. Sulfide was detected at 665 nm on a spectrometer (Spectronic 20D+, Caley & Whitmore Corp.) after coloration with dimethyl-p-phenylene,[24] and H_2O_2 was analyzed at 405 nm after coloration with $TiSO_4$.[25] Generation of new radicals in the presence of sulfite was assayed by electron spin resonance (ESR). 100 μL sample collected from the batch system without contaminants was immediately mixed with 25 μL of 0.2 M DMPO to form DMPO-radical adduct, which was then measured on a Bruker EMX ESR spectrum with microwave bridge (receiver gain, 5020; modulation amplitude, 2 Gauss;

microwave power, 6.35 mW; modulation frequency, 100 kHz; center field: 348.5 mT).

Data Analysis. Pseudo-zero-order and pseudo-first-order reaction kinetic models are used for TCE hydrodechlorination in the absence and presence of sulfite, respectively, in batch mode. Pseudo-zero-order reaction kinetics (5) is given by

$$C_t = C_0 - k_0 t \qquad (5)$$

where t is the reaction time (min), k_0 is the zero-order rate constant (μM/min), and C_0 and C_t are the concentrations (μM) at times of t = 0 and t = t, respectively. Pseudo-first-order reaction kinetics (6) is expressed as

$$ln(C_t/C_0) = -k_1 t + b \qquad (6)$$

where b is a constant and k_1 is the first-order rate constant (min^{-1}).

First-order kinetics, instead of pseudo-first-order kinetics, are successfully applied for TCE reactive transport in the column experiments, partially because the generated reactive species in the column experiments are significantly less than those generated in the well dispersed batch experiment. The one-dimensional reactive transport of TCE in the column can be modeled by the conventional advective-dispersive partial differential equation with first-order transformation kinetics:

$$\frac{\partial C(z,t)}{\partial t} - D(z,t)\frac{\partial^2 C(z,t)}{\partial z^2} + v(z,t)\frac{\partial C(z,t)}{\partial z} = -k(z,t)C(z,t), \qquad (7)$$

where $C(z,t)$ is TCE concentration in location z and time t, $k(z,t)$ stands for the first-order reaction rate, $v(z,t)$ denotes the pore water velocity, and $D(z,t)$ is the hydrodynamic dispersion coefficient. NUFT (Nonisothermal Unsaturated-saturated Flow and Transport code)[26,27], a code developed in Lawrence Livermore National Laboratory and widely applied in many applications simulating mass transfer and

reactive transport[28,29], is used to perform numerical simulations of reactive transport of TCE in columns. The details for model setup are given in Section S1 in SI.

RESULTS AND DISCUSSION

Effect of pH on TCE Hydrodechlorination and H_2O_2 Accumulation. In the presence of 1 g/L Pd/Al_2O_3, TCE was reduced in the undivided electrolytic cell in a wide pH range (Figure 2a). Control experiment shows limited removal of TCE in the absence of Pd/Al_2O_3 (Figure S3). Ethane was the main product accumulated (Inset in Figure 1a), confirming that Pd-catalytic hydrodechlorination was the dominant pathway for TCE degradation even in the presence of anodic O_2. This agrees well with previous result.[14,17] However, anodic O_2 greatly suppressed TCE hydrodechlroiantion, as evident by the much faster decay in cathodic compartment in the divided cell experiment (Figure S4). The inhibitory effect of O_2 was also revealed in Pd-catalytic hydrodechlorination studies.[6,14]

The decay of TCE in the undivided cell follows pseudo-zero-order reaction kinetics, suggesting that the rates became increasingly limited due to the availability of reactive species, chemisorbed [H] on Pd surface, with increasing reactant concentrations. Comparison of the rate constants for TCE hydrodechlorination (Table S2) demonstrates that TCE hydrodechlorination was approximate at initial pH below 4, decreased significantly with increasing initial pH from 4 to 5.5, and decreased slightly with the further increase from pH 5.5 to 10.5. This tread is different from the literature, wherein the influence of pH on TCE hydrodechlorination using H_2 under anaerobic

condition is negligible in the pH range of 4.3–11.[5,30] This difference is due to the electro-generation of O_2 and ROSs in this system.

In the undivided electrolytic system, O_2 produced at anode competes with TCE for Pd•[H].[6,14] Aside from the production of H_2O, H_2O_2 can be also be generated by the combination of chemisorbed H_2 and O_2 on Pd surface (4).[16,17,31,32] Figure 2b shows that H_2O_2 accumulation increased with decreasing pH during TCE hydrodechlorination. This suggests that H_2O_2 accumulation does not cause negative impacts on TCE hydrodechlorination. The oxidation-reduction potential (ORP) at pH 4 increased to as high as 375 mV within 80 min.[17] It is therefore feasible to supply H_2 for Pd-catalytic hydrodechlorination under electrochemically developed oxidizing condition. The simultaneous generation of H_2O_2 provides potential oxidant to increase the resistance of Pd to RSCs fouling.

Effect of Sulfide. With the increase in sulfide concentration from 0 to 93.8 μM, TCE hydrochlorination was increasingly inhibited (Figures 3a). Meanwhile, H_2O_2 production was also inhibited in a similar trend (Figure S5a). However, TCE decay always followed pseudo-zero-order kinetics, suggesting that sulfide foiled Pd catalyst by decreasing Pd•[H] generation. The trend of sulfide foiling agrees with those reported under anaerobic condition,[2,5,12,33,34] but the inhibition is much less significant compared with the literature.[5] The oxidation of sulfide using MMO electrode was reported[22–23] and was also observed in this study (Figure S6). During the course of hydrodechlorination, sulfide was not be detected in solution. Control experiment without electrolysis proves that sulfide was completely adsorbed within 2 min. Since

sulfide can be oxidized by H_2O_2 and ROSs,[20–23] it is rationale to infer that sulfide can be oxidized by the as-formed H_2O_2 and •OH on Pd surface. As a result, the resistance of Pd catalyst to sulfide foiling increased under this oxidizing condition.

Distinct Effect of Sulfite. Unexpectedly, sulfite shows a unique influence on TCE hydrodechlorination. As shown in Figure 3b, TCE degradation rate was remarkably increased when sulfite concentration increased from 0 to 1 mM. The decay deviated from pseudo-zero-order kinetics in the absence of sulfite to pseudo-first-order kinetics in the presence of sulfite（≤ 1 mM, Table S2), indicating the contribution of other reactive species in addition to Pd•[H] to TCE degradation. The total carbon decreased in the initial 40 min and increased afterwards (Figure S7), which indicates the production of undetected intermediates. The predominant production of ethane proves that hydrodechloriantion was still the dominant degradation pathway. This is different from the effect of ferrous ion, which caused a shift of dominant pathway to •OH oxidation.[17] It can be suggested that the new reactive species generated were less competitive compared with Pd•[H] and •OH. The trend of H_2O_2 accumulation was approximate at sulfite concentration less than 1 mM (Figure S5b). However in the presence of 3 mM sulfite, during the initial 60 min the degradation rate was lower than that without sulfite with negligible H_2O_2 accumulation, whereas both TCE degradation and H_2O_2 accumulation promptly increased afterwards. Sulfite was oxidized to less than 1 mM within 60 min by MMO electrodes and ROSs (Figure S8). This implies that TCE decay was enhanced when sulfite concentration decreased to less than 1 mM. The decay changed from pseudo-zero-order to pseudo-first-order

kinetics after 60 min in the presence of 3 mM sulfite, which further suggests a different degradation mechanism.

Identification of Reactive Species due to the Unique Influence of Sulfite. Enhancement of Pd-catalytic hydrodechlorination by the presence of sulfite has never been reported before. In contrast, inhibition of Pd activity for TCE hydrodechloriantion by sulfite has been well recognized under anaerobic condition.[2,5,12,13,33,34] Therefore, enhancement at low sulfite concentrations must be related to the presence of O_2 and ROSs. A series of comparison experiments were conducted to elucidate the mechanism. TCE degradation at the electrode without Pd was minute, and was even slightly suppressed by the presence of 1 mM sulfite (Figure S9). This suggests that electrode reactions as well as electro-generated H_2 and O_2 were not responsible for the enhancement. At a high pH of 10.5 without H_2O_2 accumulation, the presence of 1 mM sulfite led to marginal influence (Figure S10). And the trends of H_2O_2 accumulation at different concentrations of sulfite (Figure S5b) are similar to TCE decay (Figure 3b). Therefore, H_2O_2 probably contributed to the enhancement. However, without electrolysis TCE was negligibly degraded by H_2O_2 and 1 mM sulfite (Figure 4a), ruling out the contribution of free H_2O_2 in solution. The degradation was also minimal by H_2O_2 and 1 g/L Pd/Al_2O_3, but became significant when 1 mM sulfite was added (Figure 4a). Therefore, the combination of H_2O_2 and Pd, that is, the chemisorbed H_2O_2 and the small quantities of •OH generated from H_2O_2 decomposition on Pd surface,[16,17] is responsible for the enhancement.

The oxidation of sulfite by H_2O_2 and •OH has been extensively investigated.[18,35,36]

Sulfite can be oxidized to $SO_3^{\bullet-}$ by activated H_2O_2[35,36] and •OH (8)[37]. $SO_3^{\bullet-}$ combines with O_2 forming $SO_5^{\bullet-}$ quickly (9), which may transform to HSO_5^- at acidic condition (10) and $SO_4^{\bullet-}$ at a slow rate (11). Herein, the chemisorbed H_2O_2 and •OH are able to initiate these radical chain reactions, and the oxidizing radicals, including •OH (2.8 V/SHE), $SO_4^{\bullet-}$ (2.5–3.1 V/SHE[38]), HSO_5^- (1.82 V/SHE[37]), $SO_5^{\bullet-}$ (1.1 V/SHE[37]) and $SO_3^{\bullet-}$ (0.6 V/SHE[37]), presumably contributed to TCE decay through oxidation.

$$HSO_3^- + \bullet OH \longrightarrow SO_3^{\bullet-} + H_2O \qquad k_2 = 9.5 \times 10^9\ M^{-1}\ s^{-1}\ [37] \qquad (8)$$

$$SO_3^{\bullet-} + O_2 \longrightarrow SO_5^{\bullet-} + OH^- \qquad k_2 = 1.5 \times 10^9\ M^{-1}\ s^{-1}\ [37] \qquad (9)$$

$$SO_5^{\bullet-} + H^+ + e^- \longrightarrow HSO_5^- \qquad (10)$$

$$SO_5^{\bullet-} + HSO_3^- \longrightarrow SO_4^{\bullet-} + HSO_4^- \qquad k_2 = 3.0 \times 10^6\ M^{-1}\ s^{-1}\ [37] \qquad (11)$$

The contributions of radicals were first validated by radical scavenging experiments. Ascorbic acid is a common oxidizing radical scavenger.[39] In the presence of ascorbic acid, TCE decay was inhibited to some extent, approaching that without sulfite (Figure 4b). This proves that the oxidation pathway contributed to TCE decay in the presence of 1 mM sulfite, presumably in parallel to hydrodechlorination pathway. Methanol can effectively scavenge •OH and $SO_4^{\bullet-}$.[38] Slight inhibitory effect was observed by the addition of methanol (Figure 4b), suggesting the minute contribution of •OH and $SO_4^{\bullet-}$. The difference of the inhibition caused by ascorbic acid and methanol is assigned to the contribution of radicals with moderate oxidizing ability, i.e., $SO_5^{\bullet-}$ and $SO_3^{\bullet-}$. As $SO_3^{\bullet-}$ may react with anodic O_2 producing $SO_5^{\bullet-}$ at a diffusion-controlled rate (9)[37] and the oxidation potential of $SO_5^{\bullet-}$ is higher than that of $SO_3^{\bullet-}$,[37,41] $SO_5^{\bullet-}$ are more likely accountable for TCE oxidation.

The generation of radicals is further measured by ESR spectrum (Figure 4c). Control electrolysis experiments with 1 mM sulfite without Pd as well as with Pd without sulfite demonstrate insignificant radical signals (Curves 1 and 2). In the presence 1 mM sulfite and Pd, clear radical signals were observed (Curve 3). The feature of this radical (1:2:2:1) is similar to that of DMPO/•OH.[19] However, the contribution of •OH to TCE degradation has been verified to be minimal. ESR signals of DMPO/$SO_3^{\bullet-}$ are generally overlapped with those of DMPO/•OH, and DMPO/$SO_3^{\bullet-}$ adduct is unstable and converts to DMPO/•OH within minutes.[42,43] Therefore, the radicals generated in the presence of 1 mM sulfite can be assigned to $SO_3^{\bullet-}$ and probably small fraction of •OH. When sulfite concentration is elevated to 3 mM, the radical signals became very weak (Curve 4), due to the scavenging of oxidizing radicals by the high concentrations of sulfite.

Proposed Mechanisms for the Distinct Effects of RSCs under Oxidizing Conditions. As a consequence, the mechanisms for the influence of sulfide and sulfite are summarized in Scheme 1. At the MMO electrodes, water electrolysis produces H_2 and O_2, and both sulfide and sulfite can be oxidized to some extent. H_2 is chemisorbed on Pd surface forming atomic H, which is responsible for the efficient hydrodechlorination of TCE to ethane. Chemisorbed H_2 and O_2 on Pd surface generate H_2O_2, leading to oxidation of sulfide. Because the adsorption of sulfide on the Pd surface is quick and the oxidation of sulfide is slow, TCE hydrodechlorination by Pd•[H] is somewhat inhibited by sulfide-induced catalyst deactivation.

At low sulfite concentrations（≤ 1 mM), $SO_3^{\bullet-}$ was produced from sulfite oxidation

by chemisorbed H_2O_2 or •OH, and then quickly transformed to $SO_5^{\bullet-}$. $SO_5^{\bullet-}$ attacked the C=C bound of TCE forming TCE–$SO_5^{\bullet-}$ adduct, which was eventually hydrodechlorinated to ethane. This undetected adduct was responsible for the initial decrease of detected total carbon during TCE hydrodechlorination in the presence of 1 mM sulfite (Figure S7). As these sulfur radicals, generated from sulfite and the byproduct of H_2O_2, were less competitive compared with Pd•[H], the dominant pathway of Pd-catalytic hydrodechloriantion was almost unaffected, which is also consistent with the feature of pseudo-zero-order kinetics. Because the concentration of these radicals is dependent on sulfite and ROS concentration, the apparent decay kinetics were altered. At high sulfite concentration (3 mM), both H_2O_2 and radicals produced were quickly consumed by sulfite, and surplus sulfite foiled Pd catalyst suppressing TCE decay. When sulfite was oxidized to less than 1 mM by MMO electrode and ROSs, the pathway of radical oxidation became significant, and Pd deactivation was eliminated or alleviated.

TCE Hydrodechlorination in Three-electrode Column. A specially configured three-electrode column (Figure 1), which employs one anode (Anode) and two cathodes (Cathodes 1 and 2) to develop localized acidic and oxidizing conditions in the Pd zone, was used to evaluate the resistance of Pd to RSC foiling in flow-through mode. Because the quantity of H^+ produced at Anode is more than that of OH^- produced at Cathode 1 and the reflux of OH^- from Cathode 2 is difficult, the local low pH of about 3 in Pd zone was automatically developed (Figure S11). Therefore, generation of ROSs in the Pd zone can be anticipated. TCE degradation at Ti/MMO

electrodes without Pd (Column C1) was limited (Figure 5), which is consistent with literature.[40] When 3 g Pd/Al_2O_3 catalyst were packed (Column C2), the removals were greatly increased from 20 to 70% (Table 1), showing sharp concentration decrease within the Pd zone. The concentration decrease before Pd fillings is due to the quick mixing of pore solution in the Pd zone with the solution between Cathode 1 and Anode wherein no fillings are packed. Numerical simulation gives the decay rate constant of 0.84 min^{-1} in the Pd zone and 0.18 min^{-1} at each cathode.

In the presence of sulfide, TCE hydrodechlorination was significantly decreased (Column C4) with the rate constant of 0.21 min^{-1} in the Pd zone, implying that this column has a weak ability to resist sulfide fouling. Minimal influence of sulfite on TCE hydrodechlorination was observed (Column C3). However, the temporal variation of TCE concentrations along the column demonstrates an initially quick decrease of TCE concentration in the Pd zone, followed by an increase afterwards (Figure S12). This unique feature is consistent with the effect observed in batch experiments. Because of the much larger Pd/Al_2O_3 particles and shorter retention time in columns compared with batch, the efficiency slightly declined in later stage.

Implications. This study attempts Pd-catalytic hydrodechlorination of TCE using cathodic H_2 under electrochemically developed oxidizing conditions. It is feasible to hydrodechlorinate TCE in groundwater using cathodic H_2 even with the simultaneous evolution of O_2 and production of H_2O_2. O_2 greatly suppressed TCE hydrodechlorination, whereas H_2O_2 accumulation had minimal influence. Both H_2O_2 and MMO electrode are capable of oxidizing RSCs, increasing the resistance of Pd to

RSC fouling. In particular, sulfite can be initiated by H_2O_2 and Pd to form oxidizing radicals, providing extra contribution to TCE decay through oxidation in parallel to Pd-catalytic hydrodechlorination. This unique mechanism for the influence of sulfite was elucidated for the first time. Using a three-electrode column system, it is feasible to develop localized acidic and oxidizing conditions in the Pd zone for TCE hydrodechlorination with certain ability to resist RSC foiling. As a derivative, ROSs and electricity can inhibit microbial activity,[44,45] and acidic condition may alleviate precipitate formation from Ca^{2+}, Mg^{2+} and so on, hence having the potential to resist fouling by biofilms and precipitates.

ACKNOWLEDGEMENTS

This work was supported by the National Institute of Environmental Health Sciences (NIEHS, Grant No. P42ES017198), the Natural Science Foundation of China (NSFC, No. 41172220), and the Fundamental Research Funds for the Central Universities, China University of Geosciences (Wuhan) (No. CUGL110608). We appreciate the assistance in ESR assay by Prof. David Budil and Mr. Xianzhe Wang in Department of Chemistry & Chemical Biology, Northeastern University. The content is solely the responsibility of the authors and does not necessarily represent the official views of the NIEHS or the National Institutes of Health or Lawrence Livermore National Security, LLC.

Prepared by LLNL under Contract DE-AC52-07NA27344.

Supporting Information Available

Additional descriptions about the numerical model setup (S1); Tables S1–S2; and Figure S1–12 are provided in SI. This material is available free of charge via the internet at http://pubs.acs.org.

References

(1) Moran, M. J.; Zogorski, J. S.; Squillage, P. J. Chlorinated solvents in groundwater of the United States. *Environ. Sci. Technol.* **2007**, 41, 74–81.

(2) Chaplin, B. P.; Reinhard, M.; Schneider, W. F.; Schueth, C.; Shapley, J. R.; Strathmann, T.; Werth, C. J. A critical review of Pd-based catalytic treatment of priority contaminants in water. *Environ. Sci. Technol.* **2012**, 46, 3655–3670.

(3) He, F., Zhao, D. Hydrodechlorination of trichloroethene using stabilized Fe-Pd nanoparticles: Reaction mechanism and effects of stabilizers, catalysts and reaction conditions. *Appl. Catal. B Environ.* **2008**, 84, 533–540.

(4) Hildebrand, H.; Mackenzie, K.; Kopinke, F. D. Highly active Pd-on-magnetite nanocatalysts for aqueous phase hydrodechlorination reactions. *Environ. Sci. Technol.* **2009**, 43, 3254–3259.

(5) Lowry, G. V; Reinhard, M. Pd-catalyzed TCE dechlorination in groundwater: Solute effects, biological control, and oxidative catalyst regeneration. *Environ. Sci. Technol.* **2000**, 34, 3217–3223.

(6) Lowry, G. V; Reinhard, M. Pd-catalyzed TCE dechlorination in water: Effects of $[H_2](aq)$ and H_2-utilizing competitive solutes on the TCE dechlorination rate and product distribution. *Environ. Sci. Technol.* **2001**, 35, 696–702.

(7) Nutt, M. O.; Hughes, J. B.; Wong, M. S. Designing Pd-on-Au bimetallic nanoparticle catalysts for trichloroethene hydrodechlorination. *Environ. Sci. Technol.* **2005**, 39, 1346–1353.

(8) Yuan, G.; Keane, M. A. Aqueous-phase hydrodechlorination of 2,4-dichlorophenol over Pd/Al_2O_3: Reaction under controlled pH. *Ind. Eng. Chem. Res.* **2007**, 46, 705–715.

(9) Davie, M. G.; Cheng, H.; Hopkins, G. D.; Lebron, C. A.; Reinhard, M. Implementing heterogeneous catalytic dechlorination technology for remediating TCE-contaminated groundwater. *Environ. Sci. Technol.* **2008**, 42, 8908–8915.

(10) Schueth, C.; Kummer, N. A.; Weidenthaler, C.; Schad, H. Field application of a tailored catalyst for hydrodechlorinating chlorinated hydrocarbon contaminants in groundwater. *Appl. Catal. B Environ.* **2004**, 52, 197–203.

(11) McNab, W. W., Jr.; Ruiz, R.; Reinhard, M. In-Situ destruction of chlorinated hydrocarbons in groundwater using catalytic reductive dehalogenation in a reactive well: Testing and operational experiences. *Environ. Sci. Technol.* **2000**, 34, 149–153.

(12) Chaplin, B. P.; Shapley, J. R.; Werth, C. J. Regeneration of sulfur-fouled bimetallic Pd-based catalysts. *Environ. Sci. Technol.* **2007**, 41, 5491–5497.

(13) Angeles-Wedler, D.; Mackenzie, K.; Kopinke, F. D. Permanganate oxidation of sulfur compounds to prevent poisoning of Pd catalysts in water treatment processes. *Environ. Sci. Technol.* **2008**, 42, 5734–5739.

(14) Mcnab, JR. W. W.; Ruiz, R. Palladium-catalyzed reductive dehalogenation of dissolved chlorinated aliphatics using electrolytically-generated hydrogen.

Chemosphere **1998**, 37, 925–936.

(15) Zheng, M. M.; Bao, J. G.; Liao, P.; Wang, K.; Yuan, S. H.; Tong, M.; Long, H. Y. Electrogeneration of H_2 for Pd-catalytic hydrodechlorination of 2,4-dichlorophenol in groundwater. *Chemosphere* **2012**, 87, 1097–1104.

(16) Yuan, S. H.; Fan, Y.; Zhang, Y. C.; Tong, M.; Liao, P. Pd-catalytic in situ generation of H_2O_2 from H_2 and O_2 produced by water electrolysis for the efficient electro-Fenton degradation of rhodamine B. *Environ. Sci. Technol.* **2011**, 45, 8514–8520.

(17) Yuan, S. H.; Mao, X.; Alshawabkeh, A. N. Efficient degradation of TCE in groundwater using Pd and electro-generated H_2 and O_2: A shift in pathway from hydrodechlorination to oxidation in the presence of ferrous ions. *Environ. Sci. Technol.* **2012**, 46, 3398–3405.

(18) Hoffmann, M. R.; Edwards, J. O. Kinetics of the oxidation of sulfite by hydrogen peroxide in acidic solution. *J. Phys. Chem.* **1975**, 79, 2096–2098.

(19) Adewuyl, Y. G.; Carmlchael, G. R. Kinetics of oxidation of dimethyl sulfide by hydrogen peroxide in acidic and alkaline medium. *Environ. Sci. Technol.* **1986**, 20, 1017–1022.

(20) Chen, K. Y.; Morris, J. C. Kinetics of oxidation of aqueous sulfide by O_2. *Environ. Sci. Technol.* **1972**, 6, 529–537.

(21) Hoffmann, M. R. Kinetics and mechanism of oxidation of hydrogen sulfide by hydrogen peroxide in acidic solution. *Environ. Sci. Technol.* **1977**, 11, 61–66.

(22) Pikaar, I.; Rozendal, R. A.; Yuan, Z.; Keller, J.; Rabaey, K. Electrochemical

sulfide oxidation from domestic wastewater using mixed metal-coated titanium electrodes. *Water Res.* **2011**, 45, 5381–5388.

(23) Pikaar, I.; Rozendal, R. A.; Yuan, Z.; Keller, J.; Rabaey, K. Electrochemical sulfide removal from synthetic and real domestic wastewater at high current densities. *Water Res.* **2011**, 45, 2281–2289.

(24) Environmental Protection Administration of China, 2002. Water and Wastewater Monitoring and Analysis Methods, 4th Eds; China Environmental Science Press.

(25) Eisenberg, G. Colorimetric determination of hydrogen peroxide. *Ind. Eng. Chem. Anal. Ed.* **1943**, 15, 327–328.

(26) Nitao, J. J. *User's manual for the USNT module of the NUFT code, version 2 (NP-phase, NC-component, thermal).* Lawrence Livermore National Laboratory, UCRL-MA-130653, 1998.

(27) Hao, Y.; Sun, Y.; Nitao, J. J. *Overiew of NUFT: A versatile numerical model for simulating flow and reactive transport in porous media.* Lawrence Livermore National Laboratory, Groundwater Reactive Transport Models, 2011, 213–240.

(28) Sun, Y.; Demir, Z.; Delorenzo, T.; Nitao, J. J. *Application of the NUFT code for subsurface remediation by bioventing.* Lawrence Livermore National Laboratory, 2000, UCRL-ID-137967.

(29) Buscheck, T. A.; Sun, Y.; Chen M.; Hao, Y.; Wolery, T. J.; Bourcier, W. L.; Court, B.; Celia. M. A.; Friedmann, J. S.; Aines, R. D. Active CO_2 reservoir management for carbon storage: Analysis of operational strategies to relieve pressure

buildup and improve injectivity. *Int. J. Greenh. Gas Con.* **2012**, 6, 230–245.

(30) Munakata, N.; Reinhard, M. Palladium-catalyzed aqueous hydrodechlorination in column reactors: Modeling of deactivation kinetics with sulfide and comparison of regenerants. *Appl. Catal. B Environ.* **2007**, 75, 1–10.

(31) Edwards, J. K.; Solsona, B.; Ntainjua, N. E.; Carley, A. F.; Herzing, A. A.; Kiely, C. J.; Hutchings, G. J. Switching off hydrogen peroxide hydrogenation in the direct synthesis process. *Science* **2009**, 323, 1037–1041.

(32) Samanta, C. Direct synthesis of hydrogen peroxide from hydrogen and oxygen: an overview of recent developments in the process. *Appl. Catal. A* **2008**, 133–149.

(33) Lim, T. T.; Zhu, B. W. Effects of anions on the kinetics and reactivity of nanoscale Pd/Fe in trichlorobenzene dechlorination. *Chemosphere* **2008**, 73, 1471–1477.

(34) Schuth, C.; Disser, S.; Schuth, F.; Reinhard, M. Tailoring catalysts for hydrodechlorinating chlorinated hydrocarbon contaminants in groundwater. *Appl. Catal. B Environ.* **2000**, 28, 147–152.

(35) Ranguelova, K.; Bonini, M. G.; Mason, R. P. (Bi)sulfite oxidation by copper, zinc-superoxide dismutase: Sulfite-derived radical-initiated protein radical formation. *Environ. Health Persp.* **2010**, 118, 970–975.

(36) Mottley, C.; Mason, R. P.; Chignell, C.F.; Sivarajah, K.; Eling, T.E. The formation of sulfur trioxide radical anion during the prostaglandin hydroperoxidase-catalyzed oxidation of bisulfite (hydrated sulfur dioxide). *J. Biol.*

Chem. **1982**, 257, 5050–5055.

(37) Neta, P.; Huie, R. E. Free-radical chemistry of sulfite. *Environ. Health Persp.* **1985**, 64, 209–217.

(38) Guan, Y. H.; Ma, J.; Li, X. C.; Fang, J. Y.; Chen, L. W. Influence of pH on the formation of sulfate and hydroxyl radicals in the UV/peroxymonosulfate system. *Environ. Sci. Technol.* **2011**, 45, 9308–9314.

(39) Liang, S. X.; Zhao, L. X.; Zhang, B. T.; Lin, J. M. Experimental studies on the chemiluminescence reaction mechanism of carbonate/bicarbonate and hydrogen peroxide in the presence of cobalt(II). *J. Phys. Chem. A* **2008**, 112, 618–623.

(40) Petersen, M. A.; Sale, T. C.; Reardon, K. F. Electrolytic trichloroethene degradation using mixed metal oxide coated titanium mesh electrodes. *Chemosphere* **2007**, 67, 1573–1581.

(41) Huie, R. E.; Neta, P. Chemical behavior of $SO_3^{\bullet-}$ and $SO_5^{\bullet-}$ radicals in aqueous solutions. *J. Phys. Chem.* **1984**, 5665–5669.

(42) Li, R.; Kameda, T.; Toriba, A.; Hayakawa, K.; Lin, J. M. Determination of benzo[α]pyrene-7,10-quinone in airborne particulates by using a chemiluminescence reaction of hydrogen peroxide and hydrosulfite. *Anal. Chem.* **2012**, 84, 3215–3221.

(43) Ranguelova, K.; Rice, A. B.; Khajo, A.; Triquigneaux, M.; Garantziotis, S.; Magliozzo, R.; Mason, R. P. Formation of reactive sulfite-derived free radicals by the activation of human neutrophils: An ESR study. *Free Radical Bio. Med.* **2012**, 52, 1264–1271.

(44) Watts, R. J.; Washington, D.; Howsawkeng, J.; Loge, F. J.; Teel, A. L.

Comparative toxicity of hydrogen peroxide, hydroxyl radicals, and superoxide anion to *Escherichia coli*. *Adv. Environ. Res.* **2003**, 7, 961–968.

(45) Martínez-Huitle, C. A.; Brillas, E. Electrochemical alternatives for drinking water disinfection. *Angew. Chem. Int. Ed.* **2008**, 47, 1998–2005.

Figure captions

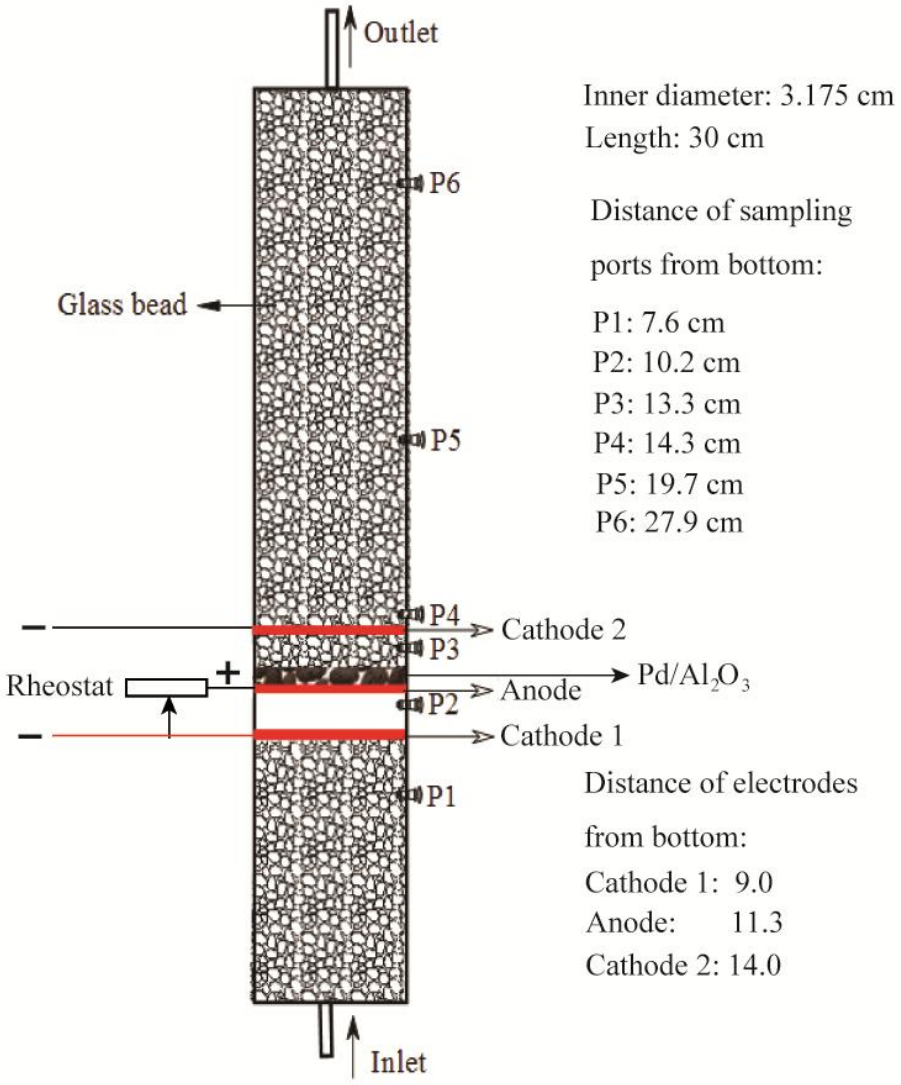

Figure 1 A schematic of three-electrode column

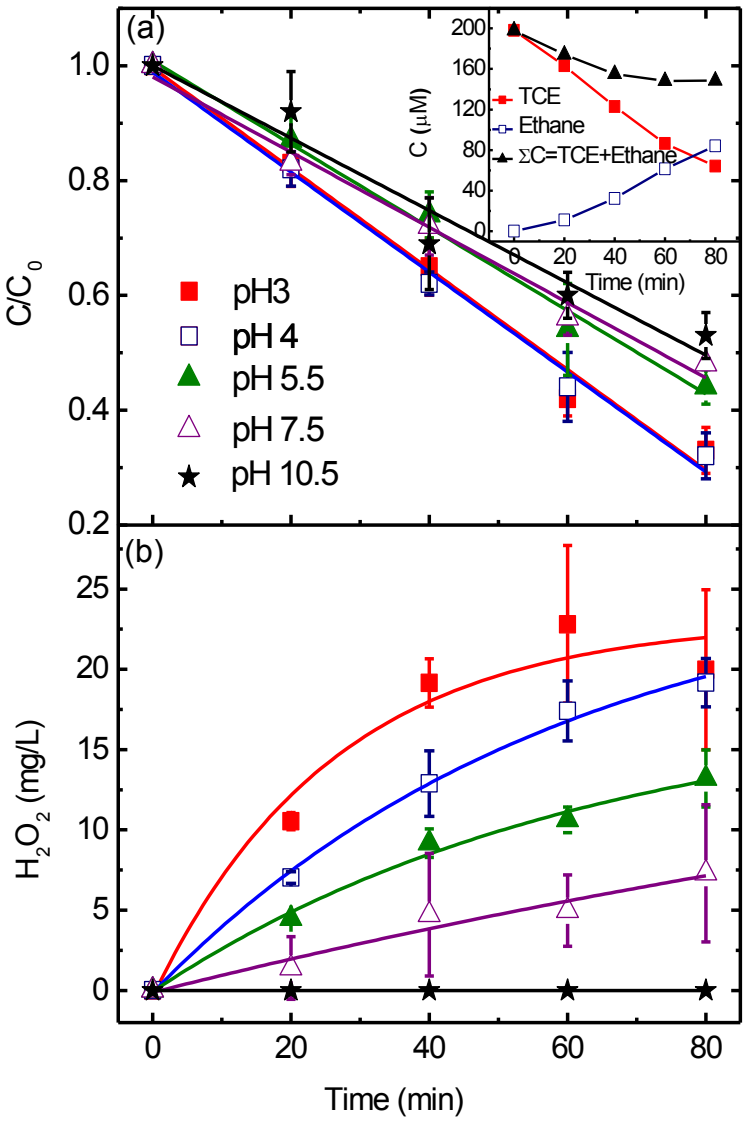

Figure 2 Effect of pH on (a) TCE hydrodechlorination and (b) H_2O_2 production. Inset graph in (a) is the degradation profile of TCE at pH 4. The degradation conditions are based on 198 μM initial TCE concentration, 1 g/L Pd/Al_2O_3 and 10 mM Na_2SO_4 background electrolyte. The pH refers to the initial solution pH. Lines in (a) refer to pseudo-zero-order kintic fittings.

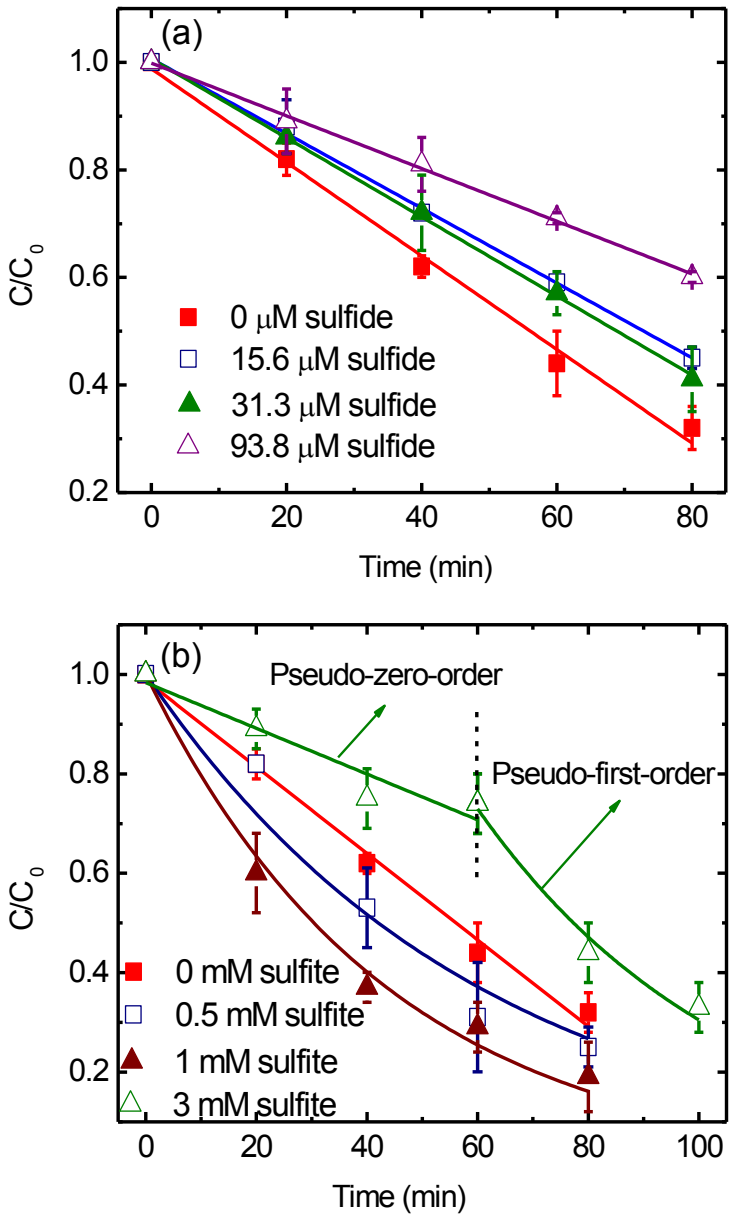

Figure 3 Effect of (a) sulfide and (b) sulfite on TCE hydrodechlorination. The degradation conditions are based on 198 μM initial TCE concentration, pH 4, 1 g/L Pd/Al_2O_3 and 10 mM Na_2SO_4 background electrolyte. Lines and curves refer to pseudo-zero-order and pseudo-first-order kintic fittings, respectively.

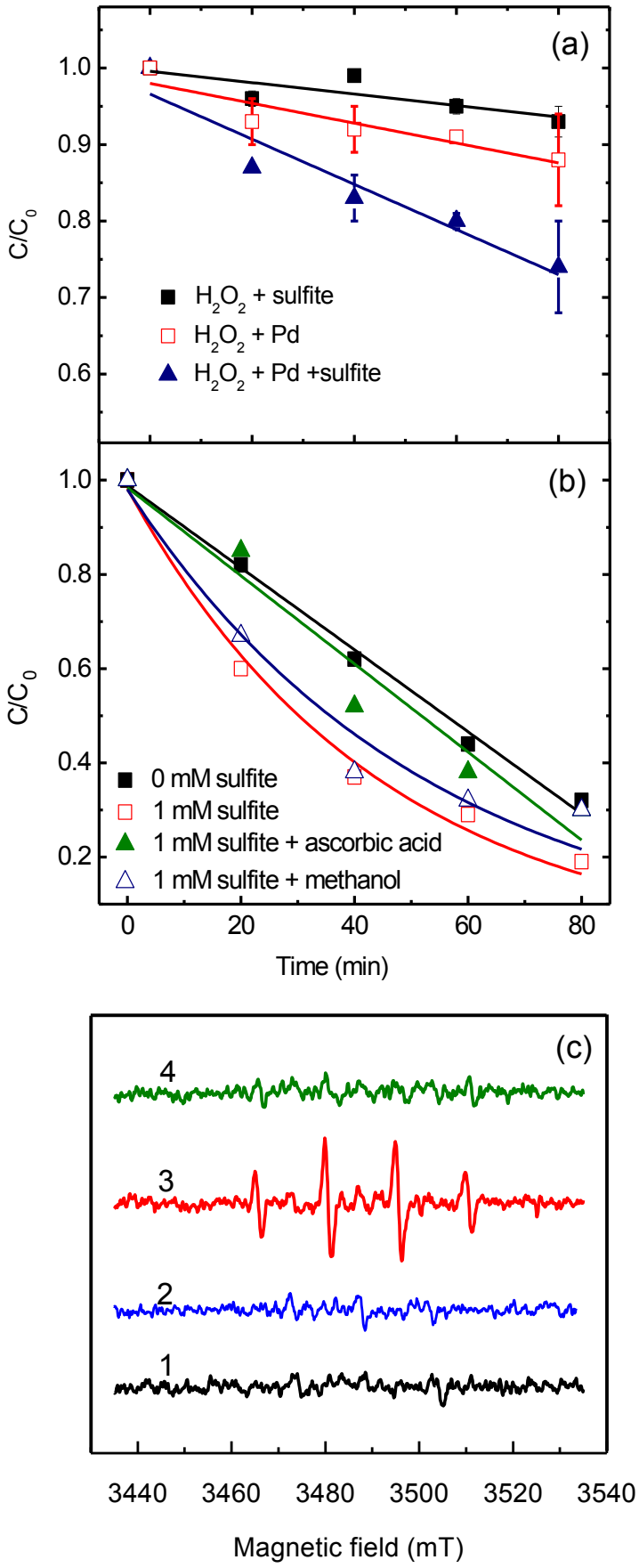

1

2 **Figure 4** (a) Effect of sulfite on TCE degradation by H_2O_2 without electricity, (b)

effect of radical scavengers on TCE degradation, (c) ESR spectra of radicals generated in the system, Curve 1: electrolysis without Pd/Al_2O_3 but with 1 mM sulfite; Curve 2: electrolysis with 1 g/L Pd/Al_2O_3 but without sulfite; Curve 3: electrolysis with 1 g/L Pd/Al_2O_3 and 1 mM sulfite; Curve 4: electrolysis with 1 g/L Pd/Al_2O_3 and 3 mM sulfite. Unless otherwised specified, the degradation conditions for (a) are based on 100 mg/L H_2O_2, 1 mM sulfite, 1 g/L Pd/Al_2O_3, pH 4 and 10 mM Na_2SO_4, for (b) based on 198 μM initial TCE concentration, pH 4, 1 g/L Pd/Al_2O_3 and 10 mM Na_2SO_4, and for (c) are based on pH 4, 100 mA, and 10 mM Na_2SO_4. The concentrations of methanol and ascorbic acid in (b) are 60 and 10 mM, respectively. Error bars in (b) are not given in order to give clear comparison.

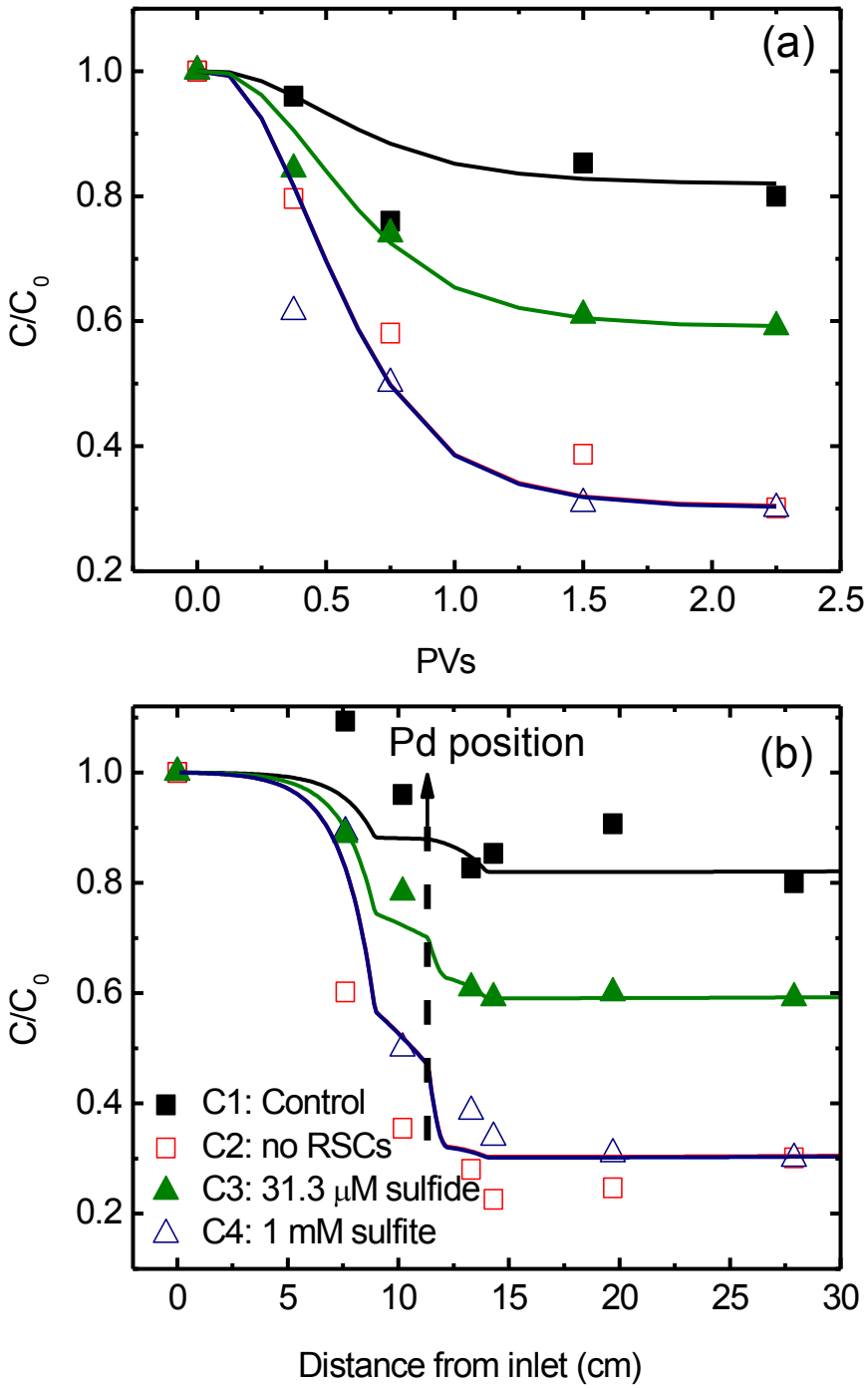

Figure 5 (a) Temporal and (b) spatial variation of TCE in columns. The spatial variation in (b) is corresponding to 2.25 PVs. See Table S1 for details of Columns C1–C4.

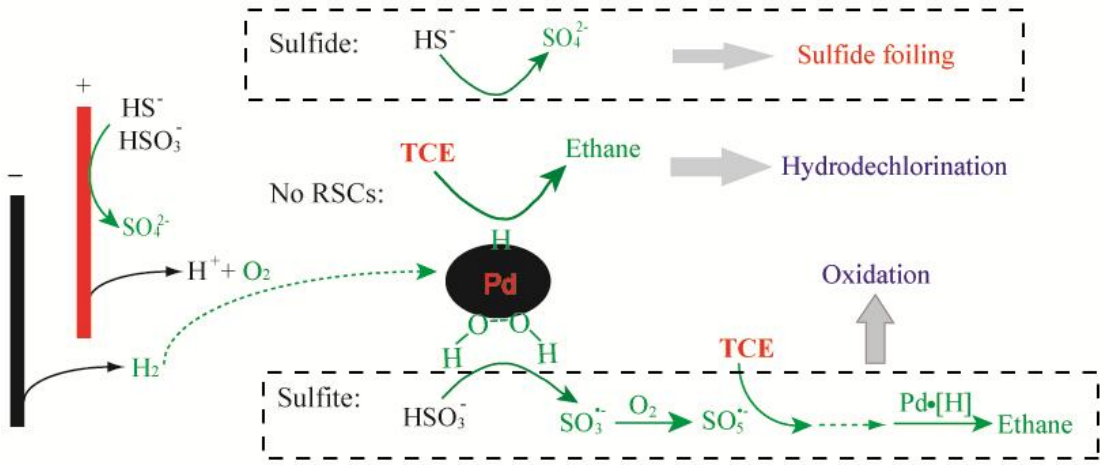

Scheme 1 Proposed mechanism for the distinct influence of sulfide and sulfite on TCE hydrodechlorination at oxidizing conditions

Supporting Information

Distinct Effects of Reduced Sulfur Compounds on Pd-catalytic Hydrodechlorination of TCE in Groundwater Using Cathodic H_2 under Electrochemically-induced Oxidizing Conditions

Songhu Yuan[†,‡]*, Mingjie Chen*[§]*, Xuhui Mao*[‡] *and Akram N. Alshawabkeh* [*,‡]

[†]State Key Lab of Biogeology and Environmental Geology, China University of Geosciences, 388 Lumo Road, Wuhan, 430074, P. R. China

[‡]Department of Civil and Environmental Engineering, Northeastern University, 400 Snell Engineering, 360 Huntington Avenue, Boston, Massachusetts 02115, United States

[§]Atmospheric, Earth and Energy Division, Lawrence Livermore National Laboratory, P.O. Box 808, L-184, Livermore, CA 94550, United States

Supporting information includes description of numerical model setup, 12 figures and 2 tables.

S1: Numerical Model Setup. NUFT (Nonisothermal Unsaturated-saturated Flow and Transport), a C++ code developed in Lawrence Livermore National Laboratory, was applied to simulate TCE reactive transport in columns. The 1-D model domain is 30-cm vertically. TCE concentration is fixed as 5.3 mg/L at the bottom boundary,

while a constant flow rate of 2 mL/min is assigned to the top boundary. The TCE concentration is initialized as 5.3 mg/L across the entire model domain. The grid resolution is 1 mm with total 300 computational cells for the 30 cm long domain. The high resolution is necessary to simulate the electrode (1.8 mm) and catalyst layer (3.2 mm), where the reactions occur, because the reaction areas dominate the spatial distribution of contaminant concentration along the column.

Based on the experiments, 0.647 and 2.65 g/cm^3 are used as porosity and density of the porous media, respectively. 1.4163×10^{-2} m of longitudinal dispersivity is obtained from conservative tracer test. Permeability is given a high value as 1.8×10^{-5} m^2 considering the 4-mm diameter of the glass bead filling. Adsorption to the glass bead is neglected in all the simulations, which was supported by the preliminary results.

With respect to reaction term, all the reactions are assumed to happen on Pd surface and at the two cathodes. Preliminary results show that TCE was reduced at cathode instead of anode in the absence of Pd catalyst. The rate constants at the two cathodes were assumed be proportional to the current partitioned. The reaction heights at each cathode and Pd catalyst are 2 mm and 7 mm, respectively. Note a length higher than experiment (3.2 mm) is used for Pd catalyst layer to account for the bubble enhancement and larger contacting area (the entire cross-section of column).

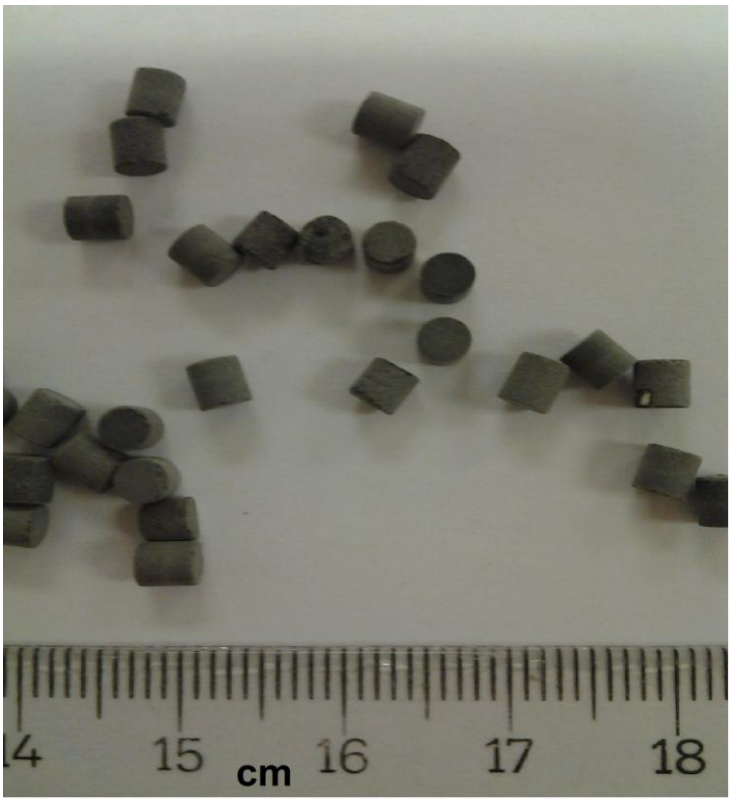

Figure S1 Pd/Al_2O_3 pellets

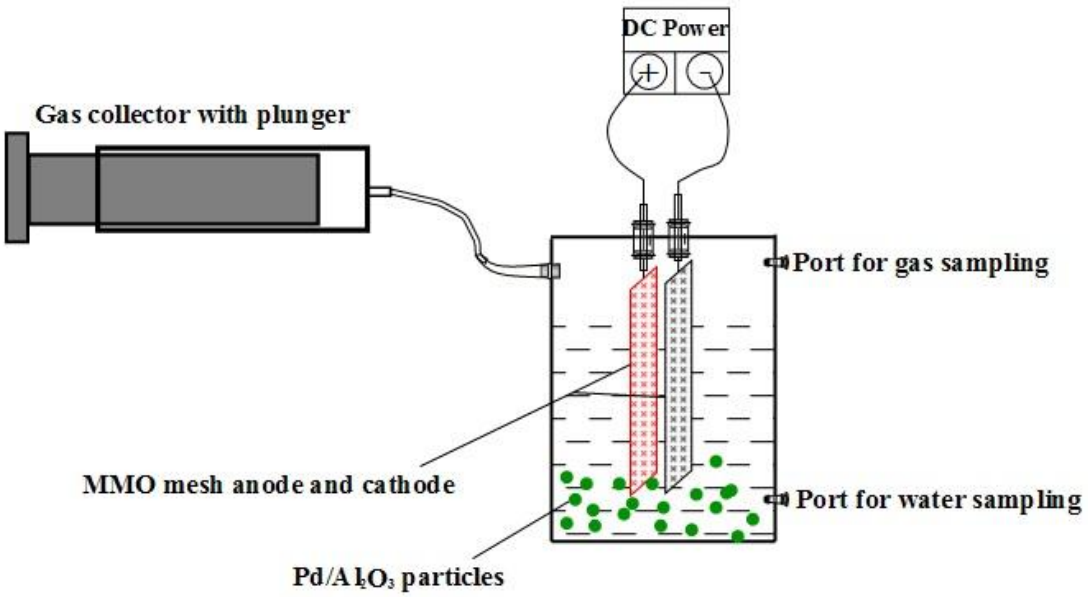

Figure S2 Batch setup for TCE degradation using H_2 generated at cathode

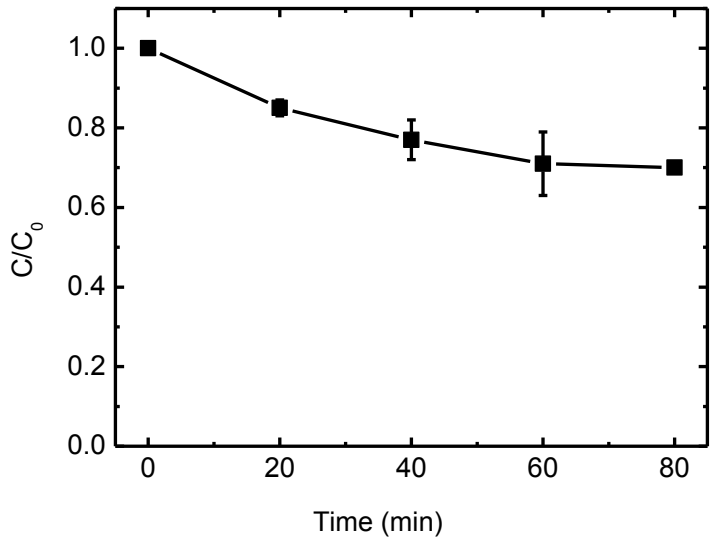

Figure S3 TCE removal in the control experiments without Pd/Al_2O_3. The degradation conditions are based on 198 μM initial TCE concentration, pH 4, 100 mA and 10 mM Na_2SO_4 background electrolyte.

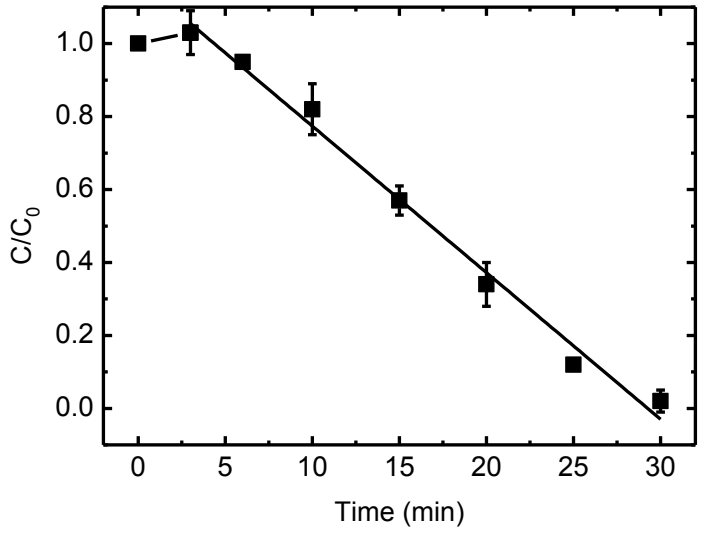

Figure S4 Pd-catalytic hydrodechloriantion of TCE in cathodic compartment in the absence of anodic O_2. The degradation conditions are based on 198 μM initial TCE concentration, pH 4, 50 mA, 1 g/L Pd/Al_2O_3 and 10 mM Na_2SO_4 background

electrolyte. The cathodic compartment is separated with anodic compartment by a Nafion membrance and has the same diameter as the undivided cell. Lines refer to pseudo-zero-order kintic fittings.

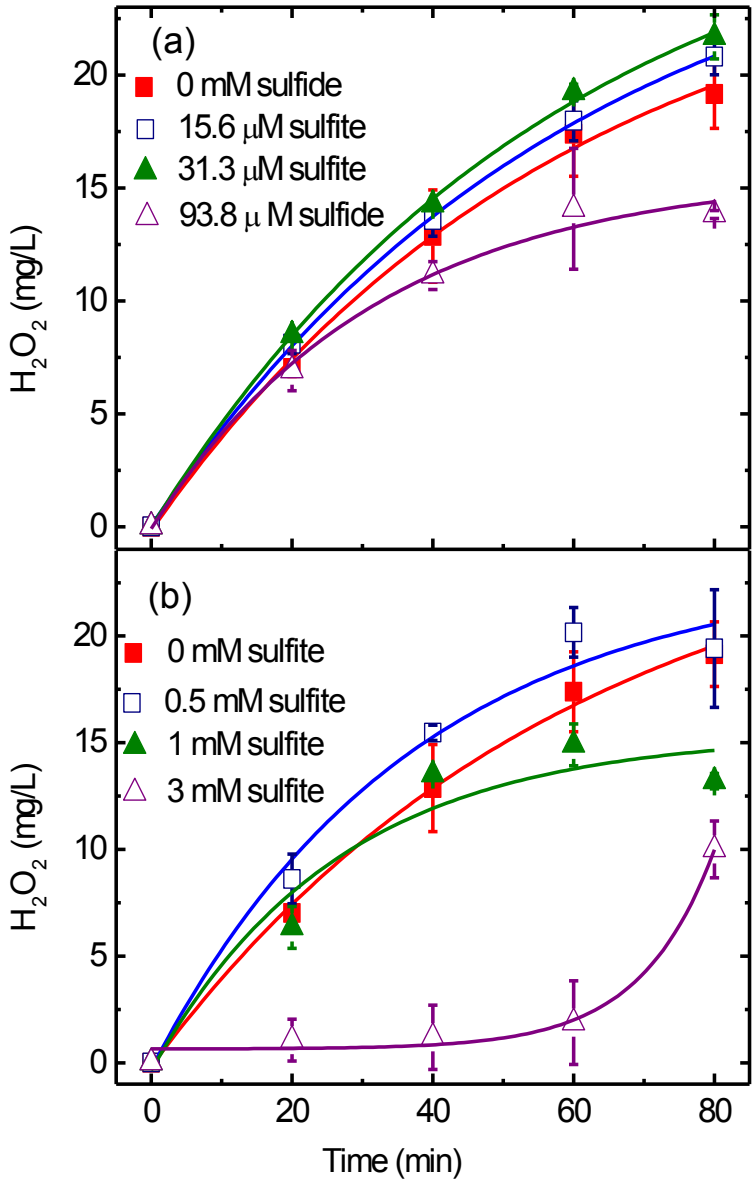

Figure S5 Effect of (a) sulfide and (b) sulfite on H_2O_2 production. The reaction conditions are based on 198 μM initial TCE concentration, pH 4, 100 mA, 1 g/L Pd/Al_2O_3 and 10 mM Na_2SO_4 background electrolyte.

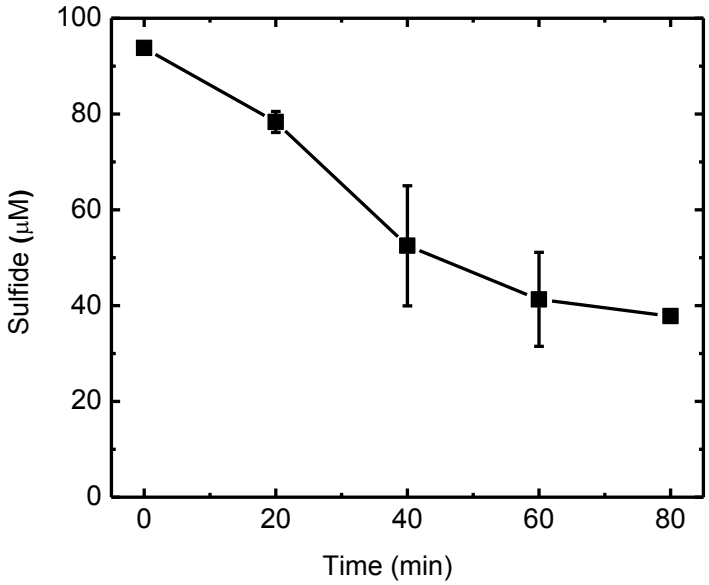

Figure S6 Electrochemcal degradation of sulfide at MMO electrode. The degradation conditions are based on 100 mA, pH 4 and 10 mM Na_2SO_4 background electrolyte.

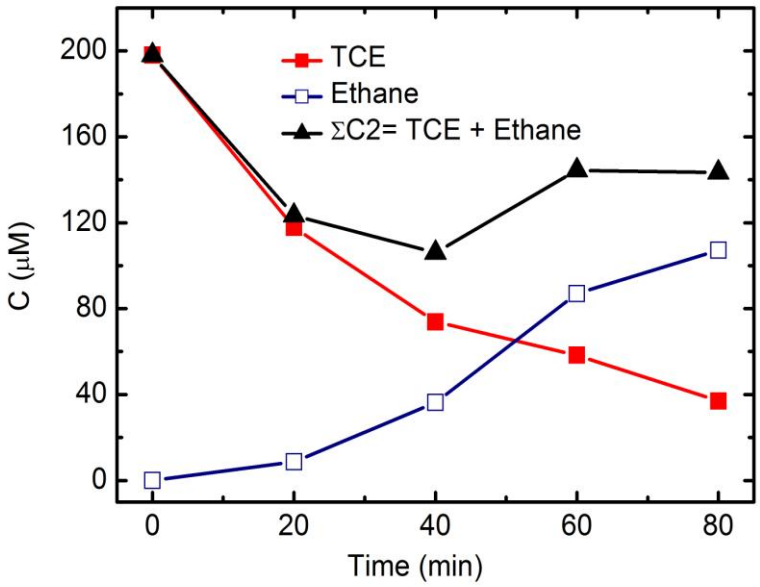

Figure S7 Mass balance for TCE hydrodechlorination in the presence of 1 mM sulfite. The degradation conditions are based on 198 μM initial TCE concentration, 100 mA, 1 g/L Pd/Al_2O_3, pH 4 and 10 mM Na_2SO_4 background electrolyte.

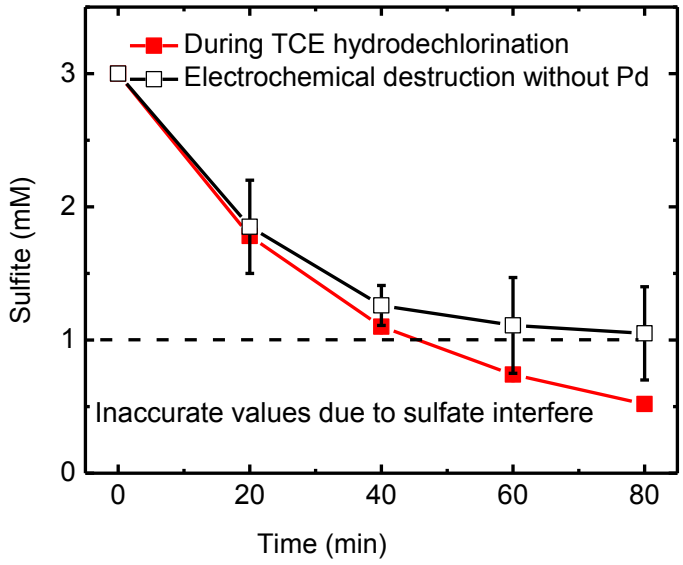

Figure S8 Variation of sulfite concentration during electrolysis. Electrochemical destruction are based on pH 4, 100 mA and 10 mM Na_2SO_4 background electrolyte. During TCE hydrodechlorination, 1 g/L Pd/Al_2O_3 and 198 μM initial TCE concentration were added.

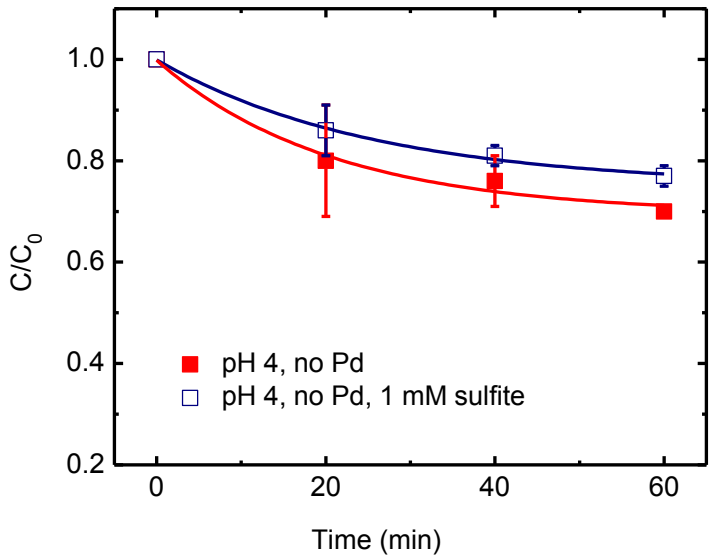

Figure S9 Influence of sulfite on electrolytic degradation of TCE at MMO electrode.

The degradation conditions are based on 198 μM initial TCE concentration, pH 4, 100 mA and 10 mM Na_2SO_4.

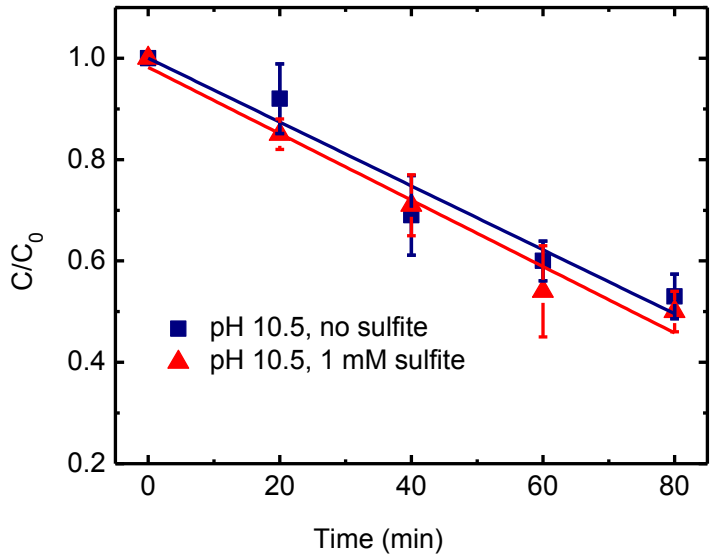

Figure S10 Effect of sulfite on TCE hydrodechlorination at pH 10.5. The degradation conditions are based on 198 μM initial TCE concentration, 100 mA, 1 g/L Pd/Al_2O_3 and 10 mM Na_2SO_4.

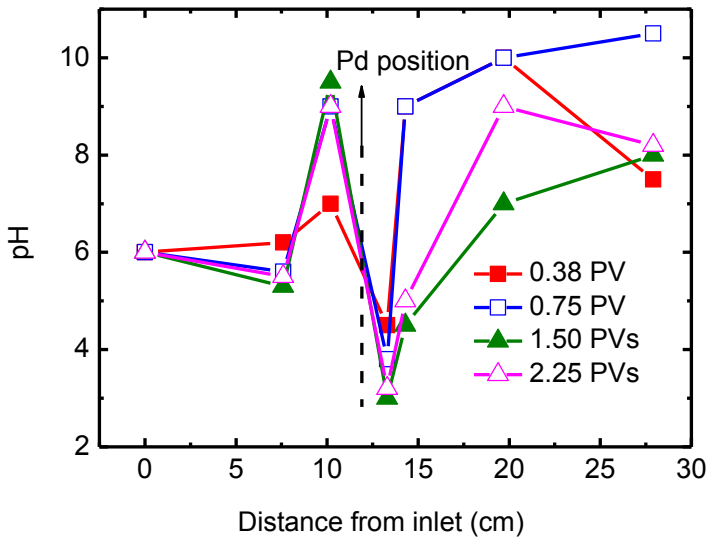

Figure S11 Variation of pH in representative three-electrode column

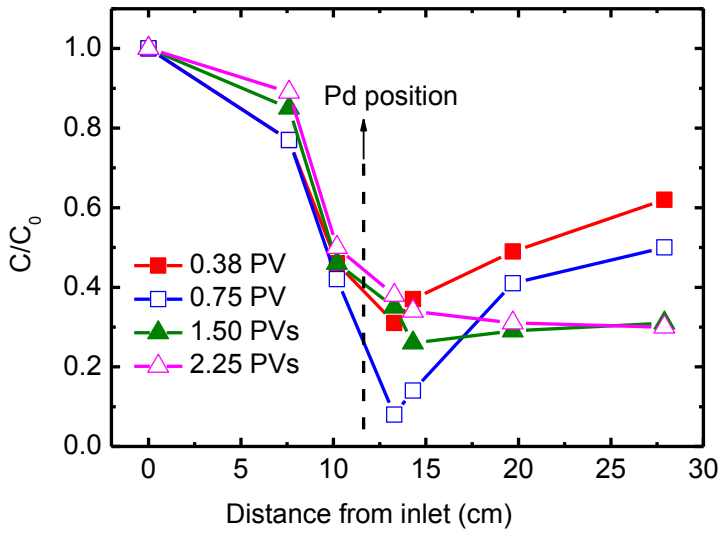

Figure S12 Temporal variation of TCE along column in the presence of 1 mM sulfite in Column C4

1

Table S1 Parameters and Results Associated with Column Experiments

no.	Groundwater composition [a]	Column description [b]	First-order rate constants k_1 (min^{-1}) [c]	Removal efficiency [d]
C1	5.3 mg/L TCE	No Pd/Al_2O_3	Cathodes 1 and 2: 0.18 Pd zone: 0	20%
C2	5.3 mg/L TCE	3 g/L Pd/Al_2O_3	Cathodes 1 and 2: 0.18 Pd zone: 0.84	70%
C3	5.3 mg/L TCE, 31.3 μM sulfide	3 g/L Pd/Al_2O_3	Cathodes 1 and 2: 0.18 Pd zone: 0.21	41%
C4	5.3 mg/L TCE, 1 mM sulfite	3 g/L Pd/Al_2O_3	Cathodes 1 and 2: 0.18 Pd zone: 0.85	70%

[a] 3 mM Na_2SO_4 and 0.5 mM $CaSO_4$ were dissolved in groundwater as background electrolytes. [b] the three electrodes were in the sequence of cathode 1, anode and cathode 2 along groundwater flow with the total current of 60 mA equally partitioned by the two cathodes. [c] First-order rate constants were obtained from simulation modeling. [c] Removal efficiency = $(C_0-C_t)/C_0 \times 100\%$, where C_0 and C_t is the influent and effluent (Port 6) TCE concentration at 2.25 PVs.

2

3

1

Table S2 Results Summarized for TCE Hydrodechlorination and H_2O_2 Accumulation in Selected Batch Experiments

no.	Variation parameters [a]	Final pH	Removal (%) [b]	H_2O_2 (mg/L) [c]	k_0 (μM/min) or k_1 (min^{-1}) [d]	R^2 for k_0 or k_1
1	pH 3.00	2.93 ± 0.01	67.2 ± 3.9	20.0 ± 5.0	k_0: 1.73 ± 0.01	0.983
2	pH 4.00	3.49 ± 0.01	67.6 ± 3.6	19.2 ± 1.5	k_0: 1.72 ± 0.01	0.991
3	pH 5.50	3.94 ± 0.03	55.7 ± 3.3	13.2 ± 1.8	k_0: 1.44 ± 0.01	0.983
4	pH 7.50	4.64 ± 0.17	51.8 ± 0.4	7.3 ± 4.3	k_0: 1.30 ± 0.01	0.984
5	pH 10.50	10.41±0.28	46.9 ± 4.4	0 ± 0	k_0: 1.25 ± 0.02	0.943
6	0 mM sulfite	3.49 ± 0.01	67.6 ± 3.6	19.2 ± 1.5	k_0: 1.72 ± 0.01	0.991
7	0.5 mM sulfite	3.22 ± 0.04	74.9 ± 4.4	19.4 ± 2.8	k_1: 0.016 ± 0.002	0.954
8	1 mM sulfite	3.15 ± 0.06	81.3 ± 6.7	13.2 ± 0.4	k_1: 0.023 ± 0.001	0.986
9 [e]	3 mM sulfite	2.84 ± 0.05	66.9 ± 5.4	8.2 ± 0.2	k_0: 0.91 ± 0.02 k_1: 0.022 ± 0.003	k_0: 0.877 k_1: 0.961
10	0 μM sulfide	3.49 ± 0.01	67.6 ± 3.6	19.2 ± 1.5	k_0: 1.72 ± 0.01	0.991
11	15.6 μM sulfide	3.65 ± 0.03	55.5 ± 2.3	20.8 ± 0.8	k_0: 1.38 ± 0.00	0.998
12	31.3 μM sulfide	3.56 ± 0.07	58.9 ± 5.9	21.7 ± 1.0	k_0: 1.46 ± 0.00	0.991
13	93.8 μM sulfide	3.71 ± 0.07	39.9 ± 0.9	13.8 ± 0.2	k_0: 0.97 ± 0.00	0.997

[a] Otherwise stated, the reaction conditions are based on 198 μM TCE, pH 4, 1 g/L Pd/Al_2O_3, 100 mA, 10 mM Na_2SO_4 and 80 min degradation. [b] Removal is the percentage of TCE reduction at 80 min. [c] The H_2O_2 concentrations refer to the final accumulated concentrations. [d] k_0 and k_1 is the

pseudo-zero-order and pseudo-first-order kinetic constant, respectively. [e] For the influence of 3 mM sulfite, the process lasts for 100 min, and the degradation in first 60 min is fitted by pseudo-zero-order kinetics and afterwards is fitted by pseudo-first-order kinetics.

1